Immunity 25, 129–141, July 2006 ©2006 Elsevier Inc. DOI 10.1016/j.immuni.2006.04.015

# Regulatory T Cells Reversibly Suppress Cytotoxic T Cell Function Independent of Effector Differentiation

Thorsten R. Mempel,[1,4] Mikael J. Pittet,[2,3,4,*] Khashayarsha Khazaie,[2,3] Wolfgang Weninger,[1] Ralph Weissleder,[2] Harald von Boehmer,[3] and Ulrich H. von Andrian[1]

[1] CBR Institute for Biomedical Research and Department of Pathology
Harvard Medical School
200 Longwood Avenue
Boston, Massachusetts 02115

[2] Center for Molecular Imaging Research
Massachusetts General Hospital and Harvard Medical School
Building 149
13th Street
Charlestown, Massachusetts 02129

[3] Dana-Farber Cancer Institute
Harvard Medical School
44 Binney Street
Boston, Massachusetts 02115

## Summary

**Mechanisms of dominant tolerance have evolved within the mammalian immune system to prevent inappropriate immune responses. $CD4^+CD25^+$ regulatory T ($T_{reg}$) cells have emerged as central constituents of this suppressive activity. By using multiphoton intravital microscopy in lymph nodes (LNs) of anesthetized mice, we have analyzed how cytotoxic T lymphocytes (CTLs) interact with antigen-presenting target cells in the presence or absence of activated $T_{reg}$ cells. Nonregulated CTLs killed their targets at a 6.6-fold faster rate than regulated CTLs. In spite of this compromised effector activity, regulated CTLs exhibited no defect in proliferation, induction of cytotoxic effector molecules and secretory granules, in situ motility, or ability to form antigen-dependent conjugates with target cells. Only granule exocytosis by CTLs was markedly impaired in the presence of $T_{reg}$ cells. This selective form of regulation did not require prolonged contact between CTLs and $T_{reg}$ cells but depended on CTL responsiveness to transforming growth factor-β. CTLs quickly regained full killing capacity in LNs upon selective removal of $T_{reg}$ cells. Thus, $T_{reg}$ cells reversibly suppress CTL-mediated immunity by allowing acquisition of full effector potential but withholding the license to kill.**

## Introduction

It has been known for more than a decade that $CD4^+CD25^+$ $T_{reg}$ cells prevent autoimmune responses by self-reactive conventional T cells (Sakaguchi et al., 1995), but the mechanisms of $T_{reg}$-mediated immunosuppression are still poorly understood. Tissue-culture experiments have shown that $T_{reg}$ cells can inhibit the activation-induced proliferation of effector T cells in a manner requiring direct cell-cell contact (Shevach, 2002). However, recent in vivo studies indicate that inhibition of effector T cell proliferation is not always necessary to achieve $T_{reg}$-dependent peripheral tolerance (Klein et al., 2003a; Lin et al., 2002). For example, in a tissue-transplant model, $T_{reg}$ cells inhibited allograft rejection but not the proliferation of alloreactive $CD8^+$ effector T cells (Lin et al., 2002). Similarly, antigen (Ag)-specific $T_{reg}$ cells and $CD8^+$ T cells proliferated massively side-by-side in Ag-draining lymph nodes (LNs) (Chen et al., 2005a). Despite the failure of $T_{reg}$ cells to limit cytotoxic T lymphocyte (CTL) proliferation in this setting, tumors expressing the cognate model Ag hemagglutinin (HA) did not undergo CTL-mediated tumor rejection, whereas tumors were effectively eliminated when CTLs were activated in the absence of HA-specific $T_{reg}$ cells (Chen et al., 2005a). The activated $T_{reg}$ cells exerted this suppressive activity by preventing $CD8^+$ T cells from becoming cytotoxic in the draining LN (Chen et al., 2005a). Although the reasons for this $T_{reg}$ cell-induced impairment of cytotoxicity have not been determined, a number of mechanisms are conceivable, including defects in CTLs due to: altered migratory properties; inability to recognize or to form conjugates with Ag-bearing target cells; lack of cytotoxic effector molecules; failure to assemble or exocytose lytic granules; or any combination thereof.

Here we have systematically explored each of these candidate suppressor mechanisms by directly visualizing the interactions of CTLs and Ag-presenting target cells as well as $T_{reg}$ cells in situ. To this end, an established model to study CTL responses against a subcutaneously injected HA-expressing tumor cell line (Chen et al., 2005a) was adapted to perform multiphoton intravital microscopy (MP-IVM) in Ag-draining LNs of anesthetized mice (Mempel et al., 2004). We found that primed CTLs migrate normally and respond to encounter of Ag-presenting target cells in LNs by forming stable conjugates in the absence or presence of $T_{reg}$ cells. However, the ability of regulated CTLs to induce target cell lysis was greatly impaired. Ex vivo analysis of CTLs showed that failure to kill target cells in vivo was correlated with impaired release of lytic granules, while cellular granule content and endowment with lytic effector molecules was unchanged. Suppression depended on transforming growth factor-β (TGF-β) signaling in CTLs and was reversible upon in vivo removal of $T_{reg}$ cells after CTL priming, but did not require prolonged physical interactions of CTLs with $T_{reg}$ cells. These observations indicate that $T_{reg}$ cells can reversibly blunt T cell responses by selectively modulating a terminal effector function of primed $CD8^+$ T cells.

## Results

### Imaging Apoptosis of Target B Cells In Vivo

To induce CTL differentiation in situ, a small number ($1 \times 10^5$) of naive transgenic $CD8^+$ T cells expressing enhanced green fluorescent protein (EGFP) and a T cell

*Correspondence: mpittet@hms.harvard.edu

[4] These authors contributed equally to this work.

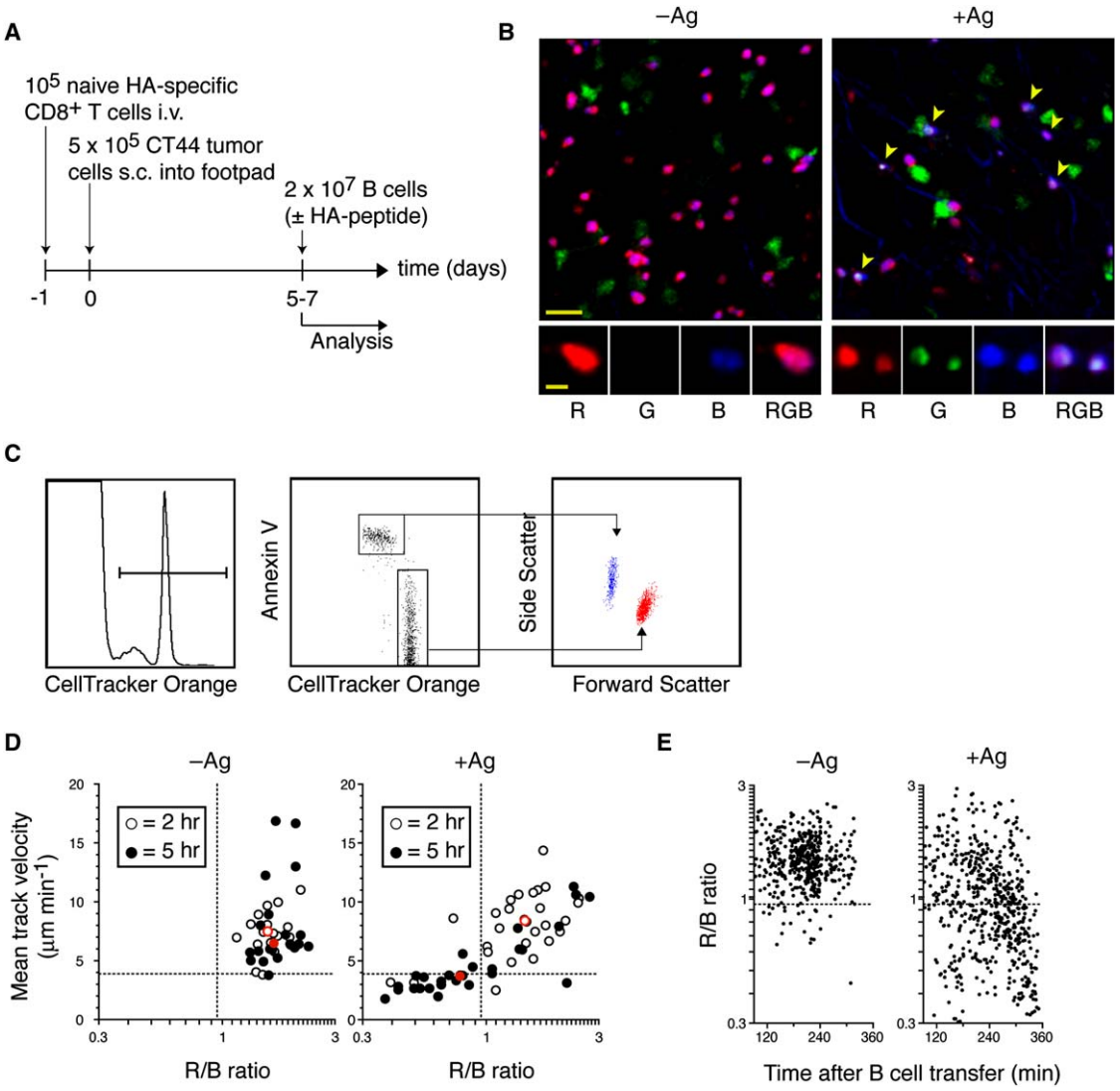


Figure 1. CTL-Mediated Killing of Ag-Pulsed B Cells Can Be Monitored through Changes in Motility and the R/B Fluorescence Intensity Ratio

(A) Experimental protocol. BALB/c mice received intravenous injections of HA-specific EGFP$^+$ transgenic CD8$^+$ T cells, followed by implantation of HA-expressing tumors into the right footpad. 5–7 days later, B cells were fluorescently labeled with CMTMR and Hoechst33342. Labeled antigen-pulsed or unpulsed B cells were injected i.v. and CTL activity was monitored in the tumor-draining LN.

(B) MP-IVM micrographs of tumor-draining LNs 4 hr after injection of unpulsed (left) or Ag-pulsed (right) B cells. Arrows identify killed B cells, i.e., immotile cells with reduced red-to-blue fluorescence ratios (scale bar equals 20 μm). Bottom panels show merged and single-color fluorescent images of representative live (left) and killed (right) B cells (scale bar equals 5 μm).

(C) Ag-pulsed B cells labeled with CMTMR (CellTracker Orange) were harvested from tumor-draining CTL-containing LNs 6 hr after injection, stained with Annexin V, and analyzed by flow cytometry.

(D) Unpulsed (left) and Ag-pulsed (right) B cells in tumor-draining LNs were analyzed for R/B intensity ratios and mean track velocities at 2 hr (empty symbols) and 5 hr (filled symbols) after i.v. injection. Medians are shown in red and are not statistically different in absence of Ag (R/B ratio of 1.54 versus 1.64, p = 0.18, and velocity of 7.47 versus 6.46 μm/min, p = 0.30, for 2 and 5 hr) but differ in presence of Ag (R/B ratio of 1.47 versus 0.78, p = 0.0021, and velocity of 8.50 versus 3.83 μm/min, p = 0.0001, for 2 and 5 hr). Thresholds separating viable from dead cells (dashed lines) were defined as described in Experimental Procedures.

(E) Unpulsed (left) and Ag-pulsed B cells (right) were analyzed in tumor-draining LNs for R/B ratios from 90 to 360 min after i.v. injection. Each data point represents an individual B cell; data were pooled from 7 (−Ag) or 8 (+Ag) recordings in three independent experiments per group.

receptor (TCR) recognizing an epitope from influenza virus-derived HA in H-2K$^d$ (Morgan et al., 1996) were adoptively transferred to BALB/c recipients (Figure 1A). It has been shown previously that subsequent footpad implantation of HA-transduced CT44 colon carcinoma cells (Klein et al., 2003b) as a continuous source of Ag induces massive expansion of HA-specific donor T cells in the draining popliteal LN (popLN). The activated cells eventually give rise to highly cytotoxic effectors, leading to macroscopic tumor shrinkage from day 7 onward. HA peptide-pulsed splenocytes obtained from BALB/c mice and adoptively transferred on day 6 after tumor implantation are rapidly eliminated in tumor-draining popliteal LN (popLN), indicating that full-fledged CTLs specific for the tumor-expressed HA arise in this LN prior to their peripheralization (Chen et al., 2005a).

We modified this model for MP-IVM analysis of intranodal CTL function: on day 5 after tumor implantation, purified B cells were adoptively transferred after differential fluorescent labeling of DNA and cellular proteins with Hoechst33342 (blue) and CMTMR (red), respectively. This staining protocol was based on the expectation that lysed cells would lose soluble cytoplasmic (red) proteins, whereas the Hoechst33342 emission would increase as nuclei become apoptotic (Kohler et al., 2003). The double-stained B cells homed avidly to popLNs and mingled in the superficial paracortex with EGFP-expressing CTLs (see Movies S1 and S2 in the Supplemental Data available with this article online). Whereas Ag-free control B cells retained their blue and red fluorescence and were highly motile, an increasing fraction of HA-peptide-pulsed B cells became immotile and underwent a dramatic change in appearance; they became visibly smaller and lost most of their red fluorescence while gaining in blue intensity (Figure 1B and Figure S1). Many immotile B cells also emitted detectable green fluorescence, presumably due to spectral overlap of the more intense Hoechst33342 emission at wavelengths detected through the green channel (525/50 nm), which was not observed with motile B cells. Thus, when red, green, and blue channels were merged, the motile control B cells had a reddish-purple color while most immotile Ag-pulsed B cells appeared bluish-white. Flow cytometric analysis of Ag-pulsed donor B cells in single-cell suspensions of CTL-containing recipient popLNs revealed that the loss of red fluorescence was invariably associated with cell death (Figure 1C). When B cell fate was monitored over the first 6 hr after adoptive transfer, control B cells always exhibited high motility and a constant red-to-blue fluorescence intensity ratio (henceforth called R/B ratio; see Experimental Procedures), whereas the Ag-pulsed target cells gave rise to a progressively larger stationary population of nonviable cells with low R/B ratios (Figures 1D and 1E).

### Kinetics of CTL-Target Cell Encounters In Vivo

Having determined that motility in conjunction with the R/B ratio are empirical indicators of B cell viability in situ, we performed MP-IVM to investigate how $EGFP^+$ CTLs interact with their targets. The CTLs rapidly formed stable conjugates with viable Ag-pulsed B cells (Figure 2A), but they made only transient contacts with unpulsed B cells (Figures 2A and 2C and Movie S2). Curiously, CTLs appeared to be able to discern live from dead victims; more than 95% of newly formed stable contacts with Ag-pulsed targets involved live B cells, whereas CTLs ignored dead B cells even when they had been killed only minutes earlier. Conjugate formation with live targets was typically followed by a period during which monogamous CTL-B cell pairs migrated together, with B cells always leading the way (Movie S3), similar to what has been described for antigen-stimulated B cells receiving help from $CD4^+$ T cells (Okada et al., 2005). Because it is not possible to measure the intercellular forces during these encounters, we can not determine whether CTLs were pushing the B cells or whether the B cells were dragging the CTLs. It should be noted, however, that the microtubule-organizing center (MTOC) in interacting T cells has been shown to polarize toward the contact site during a stable contact with an APC (Dustin et al., 1997; Stinchcombe et al., 2001b). One might speculate that this polarization may preclude simultaneous migration on a substrate other than the APC to which the CTL is attached, since in migrating lymphocytes, the MTOC is typically located at the trailing end of the cell relative to the nucleus. The initial high motility phase of CTL-B cell conjugates was followed after ~10 min by sometimes gradual and sometimes abrupt slowing of the conjugates ending in complete immotility. Conjugate arrest was seen in 71% of all interactions that could be observed from beginning to end; in a minority of conjugates (29%), the CTLs disengaged from apparently intact B cells (Figure 2B). B cell arrest was invariably followed within ~10 min by a sudden drop in R/B ratio, which was occasionally preceded, but in most cases followed by, detachment of the CTL (Figures 2A and 2C–2E). In several instances, we recorded sudden protrusions of red fluorescent material from B cells undergoing cytolysis reminiscent of membrane blebbing, which has been observed when cells are killed in vitro (Stinchcombe et al., 2001b). Because of the high B cell motility, limited size of the observed lymph node volume, and limited duration of recordings (60 min), a few intact B cells that disengaged from CTLs (n = 9) might have died after they migrated out of the field of observation or after the recording ended. If this was the case, one would have expected to observe also B cells that migrate into the field of view and, without observed contact to a CTL, arrest and lose structural integrity. We have recorded three such events during 8 hr of continuous observation and, therefore, cannot exclude the possibility that a fraction (~1/3) of B cells that remain intact after CTL dissociation might eventually die unobserved.

The average time interval between contact initiation and overt signs of structural target cell damage (17 ± 7 min, ranging from 9 to 25 min) in this in vivo setting was longer than what has been reported for CTL lysis in vitro (Stinchcombe et al., 2001b). However, it is likely that irreversible cytotoxic damage was incurred already when target B cells underwent migratory arrest. Moreover, the CTLs were remarkably efficient; within 6 hr after antigen-pulsed B cell injection, very few viable target cells were left in CTL-containing LNs. Instead, MP-IVM recordings at late time points after B cell transfer revealed a conspicuous population of condensed, irregularly shaped aggregates of red and blue fluorescent material, which became more frequent over time and were not seen when control B cells were infused. These objects probably represented phagolysosomes of macrophages or dendritic cells that had ingested fluorescent material from lysed target cells (Movie S4).

### $T_{reg}$ Cells Impair CTL Lytic Function, but Not Conjugate Formation with Target Cells

Having established an MP-IVM approach to visualize and analyze the kinetics and efficacy of CTL-mediated target cell killing, we asked how the presence of activated $T_{reg}$ cells affects CTL function. Coadoptive transfer of HA-specific $T_{reg}$ cells with HA-specific $CD8^+$ T cells followed by implantation of CT44 tumors results in clonal expansion of both T cell populations, but the ensuing CTLs fail to reject the tumors (Chen et al., 2005a). Accordingly, regulated CTLs that developed in popLNs

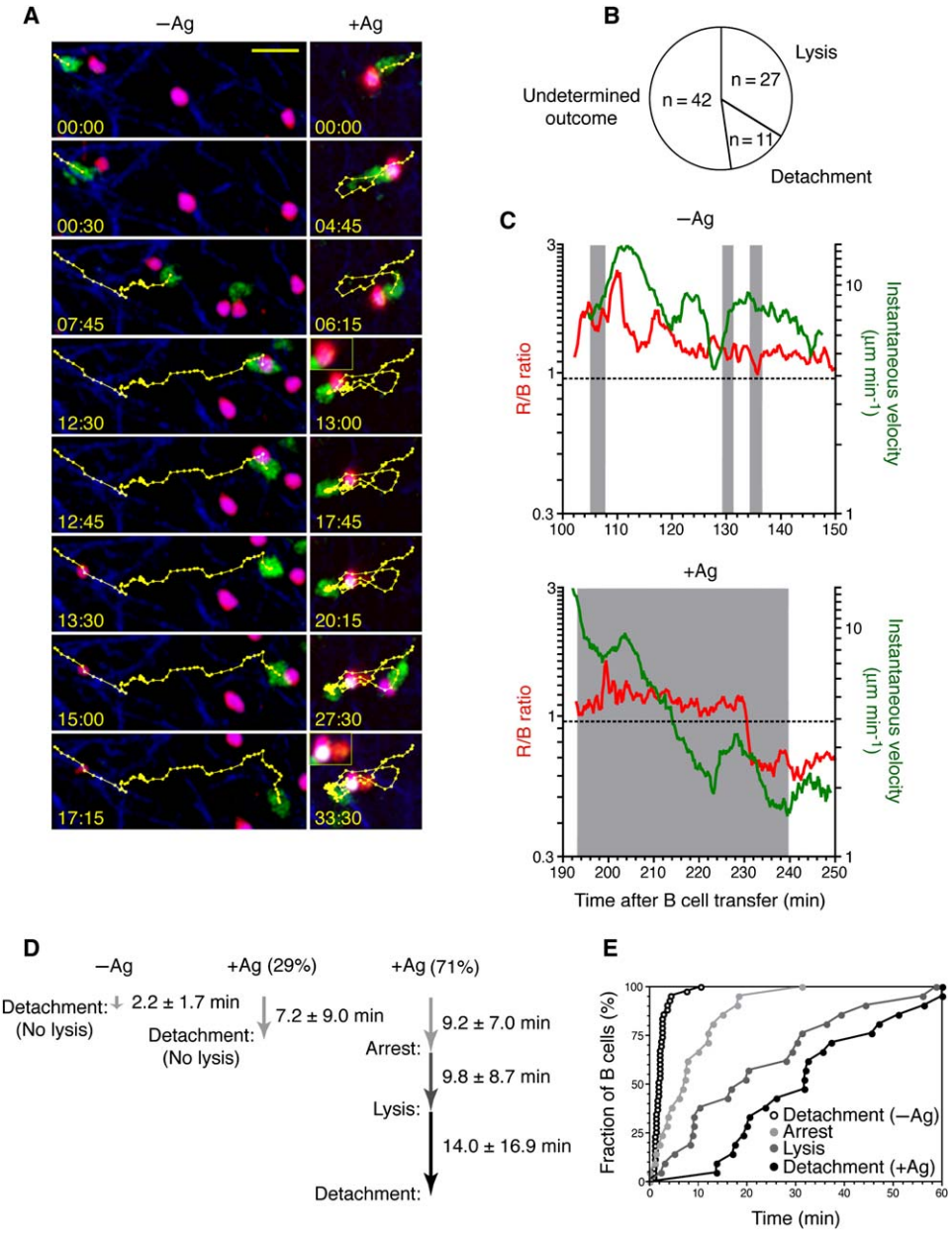


Figure 2. Sequential Steps during Killing of Ag-Pulsed B Cells by CTLs

(A) Ag-free B cells (red/purple) are scanned by a CTL (green) in a series of short-lasting contacts (left). The time interval from the beginning of each recording is shown as minutes and seconds. Upon encounter with an Ag-pulsed B cell (right), a CTL forms a stable, motile conjugate with its target. At 13 min, the conjugate becomes permanently arrested, but B cell color is still unchanged (inset). A color change in the B cell indicative of loss of structural integrity is first apparent after ~20 min and remains visible until the end of the recording at 33:30 min, at which time the lysed cell has extruded a prominent membrane bleb (inset). Yellow dots track the position of the CTL's centroid at 15 s time intervals (scale bar equals 20 μm). The still images of CTL-B cell interactions without and with Ag are from Movies S2 and S3, respectively.

(B) Outcome of 80 individual CTL-B cell interactions from four independent experiments. "Lysis" defines B cells with a R/B ratio that dropped below 0.95 after CTL interaction (see Experimental Procedures), "detachment" defines B cells that detached from CTLs and retained an R/B ratio above 0.95, and "undetermined outcome" defines CTL-B cell conjugates that left the recorded region before lysis or detachment could be observed.

(C) Single-cell recordings of time-averaged migratory velocity (green line) and R/B ratio (red line) as parameters of viability of B cells during encounters with CTLs (gray bars). Transient encounters of unpulsed B cells with CTLs did not alter either parameter, whereas Ag-pulsed B cells first became immotile and, subsequently, their R/B ratio dropped below the viability threshold (dashed line).

(D) Mean duration of the different phases of B cell interactions with CTLs. Light gray arrows reflect motile interactions until either detachment or motility arrest; dark gray arrows show time from motility arrest to structural lysis; black arrow reflects time from structural lysis to detachment of the CTLs. Numbers on the right show the mean duration (± SD) of each phase in minutes.

(E) Data from (D) plotted as cumulative frequency histogram.

in the presence of HA-specific $T_{reg}$ cells failed to kill Ag-pulsed B cells (Figure 3A). However, B cells interacting with regulated CTLs became much less frequently immotile. Instead, the B cell-CTL couples continued to migrate vigorously. Eventually, most interactions were terminated by detachment of the regulated CTLs or, owing to the long duration and dynamic nature of the interactions, the migrating conjugates left the imaged tissue volume (Figures 3B–3D and Movie S5). Both regulated and nonregulated CTLs had the same gross distribution within popLNs, displayed equivalent migratory activity (Figure S2 and Movie S5), polarized similarly toward target B cells during the motile interaction phase (Figure S2), and efficiently formed stable conjugates with their targets (95.8% and 94.7% interactions with Ag-pulsed B cells and regulated or unregulated CTLs, respectively, lasted for >3 min; in comparison, the upper 95% CI of mean for interactions with control unpulsed targets was 2.7 min, data not shown and Figure 3E).

In comparison to nonregulated CTL-B cell conjugates, Ag-pulsed B cell conjugates with regulated CTLs that could be followed from beginning to end (26% of all conjugates observed) lasted twice as long before either detaching (17%) or, less frequently, resulting in B cell death (Figure 3E). In the few cases in which regulated CTLs induced B cell arrest (9%), the time required for subsequent loss of the target's structural integrity and eventual detachment of the CTLs was the same as with nonregulated CTLs, suggesting that these late steps in the killing process were not influenced by $T_{reg}$ cells (Figure 3E). However, because regulated CTL-B cell conjugates persisted longer and resulted less frequently in a "lethal hit," there was a 6.6-fold difference in the frequency of killing events during the total observed time of motile CTL-B cell conjugation; the hourly kill rate was 2.42/hr and 0.36/hr in the absence and presence of $T_{reg}$ cells, respectively (Figure 3F). Thus, $T_{reg}$ cell-mediated CTL suppression in LNs does not interfere with $CD8^+$ T cell expansion, distribution, or motility, nor does it affect the CTL's ability to detect agonist TCR ligands on B cells or to form antigen-specific stable conjugates. Suppression in this setting appears to manifest itself exclusively in compromised lytic activity.

### Regulated CTLs Are Sufficient in Content but Not Release of Lytic Granules

When $CD8^+$ T cells differentiate into CTLs, they assemble specialized secretory granules that store cytotoxic effector molecules. Cytolysis requires the translocation and exocytosis of these lytic granules at the CTL-target cell interface, where the granule contents are endocytosed by the target and then trigger several proapoptotic pathways (Lieberman, 2003; Trapani and Smyth, 2002). Despite the dramatic difference in cytotoxic potential, the size, number, and subcellular distribution of lytic granules in regulated and nonregulated CTLs was virtually identical (Figures 4A and 4B). Likewise, we found no difference between regulated and nonregulated CTLs in mRNA expression of multiple effector molecules (Figure 4C) or the transcription factors T-bet and eomesodermin, which are required for optimal CTL differentiation (Pearce et al., 2003; Sullivan et al., 2003) (data not shown). The expression of lytic effector molecules may also be regulated posttranscriptionally. We could not assess perforin content in CTLs due to lack of an adequate mAb and/or staining protocol for specific staining, yet we found no significant difference between regulated and nonregulated CTLs in granzyme B content (Figure S6). However, the diminished cytolytic activity of regulated CTLs correlated with a marked delay and decreased frequency in activation-induced degranulation, as determined by mobilization of the lysosomal marker CD107a to the cell surface upon encounter with Ag-presenting cells (Figure 5A and Figure S3). Degranulation of regulated CTLs was strongly impaired (between 75% and 95% decrease) during the first 30 min after Ag challenge. This early impairment of degranulation may be particularly important because our in vivo observations indicate that CTLs have a constrained window of opportunity to induce target cell death before conjugates dissociate (>95% motile interactions last for less than 30 min, mean ± SD, 8.4 ± 7.2 min). Thus, impaired granule exocytosis is a plausible mechanism for the failure of regulated CTLs to eliminate target cells to the extent observed in vivo.

### CTL Suppression Depends on TGF-β Signaling

How might $T_{reg}$ cells modulate the effector function of intranodal CTLs? In many settings, undesired self-targeted immune responses are suppressed by TGF-β (Gorelik and Flavell, 2002). Recent work indicates that $T_{reg}$ cells are relatively poor producers of this cytokine, but they have been suggested to function in a TGF-β-dependent fashion by inducing TGF-β production by other cells (Kullberg et al., 2005). Indeed, TGF-β also plays a role in the present model; HA-specific CTLs that expressed a dominant-negative TGF-β type II receptor (dnTGFβRII) (Gorelik and Flavell, 2000) displayed similar kinetics of expansion as wild-type CTLs and displayed comparable cytotoxic activity, but they efficiently eliminated HA-expressing tumors even when $T_{reg}$ cells were present. Thus, although there are other mechanisms by which $T_{reg}$ cells can exert immunosuppressive activities (Shevach, 2002), responsiveness to TGF-β is prerequisite to CTL suppressibility in this model (Chen et al., 2005a). Indeed, when HA-specific dnTGFβRII CTLs were harvested from popLNs on day 6 or 7 after tumor implantation, they degranulated rapidly upon restimulation regardless of whether they were generated in the presence or absence of $T_{reg}$ cells, indicating that compromised cytotoxicity and impaired degranulation depend on TGF-β (Figure 5B). In contrast, the mere addition of TGF-β to cultures of nonregulated CTLs was not sufficient to block degranulation acutely (data not shown). Thus, other suppressive signals generated by $T_{reg}$ cells and/or other cells may be needed for CTL regulation.

### Suppression of CTLs Is Reversed upon Removal of $T_{reg}$ Cells

Next, we asked whether $T_{reg}$ cell-mediated suppression of CTLs is reversible. Congenic $Thy1.2^+$ CTLs and $Thy1.1^+$ $T_{reg}$ cells were allowed to proliferate in CT44 tumor-bearing $Thy1.2^+$ hosts. On days 5 and 6, at a time when virtually all HA-specific $CD8^+$ T cells had been activated and induced to proliferate in popLNs, the $T_{reg}$ cells were selectively depleted by anti-Thy1.1 mAb injection (Figure 6A). 2 days after $T_{reg}$ cell depletion,

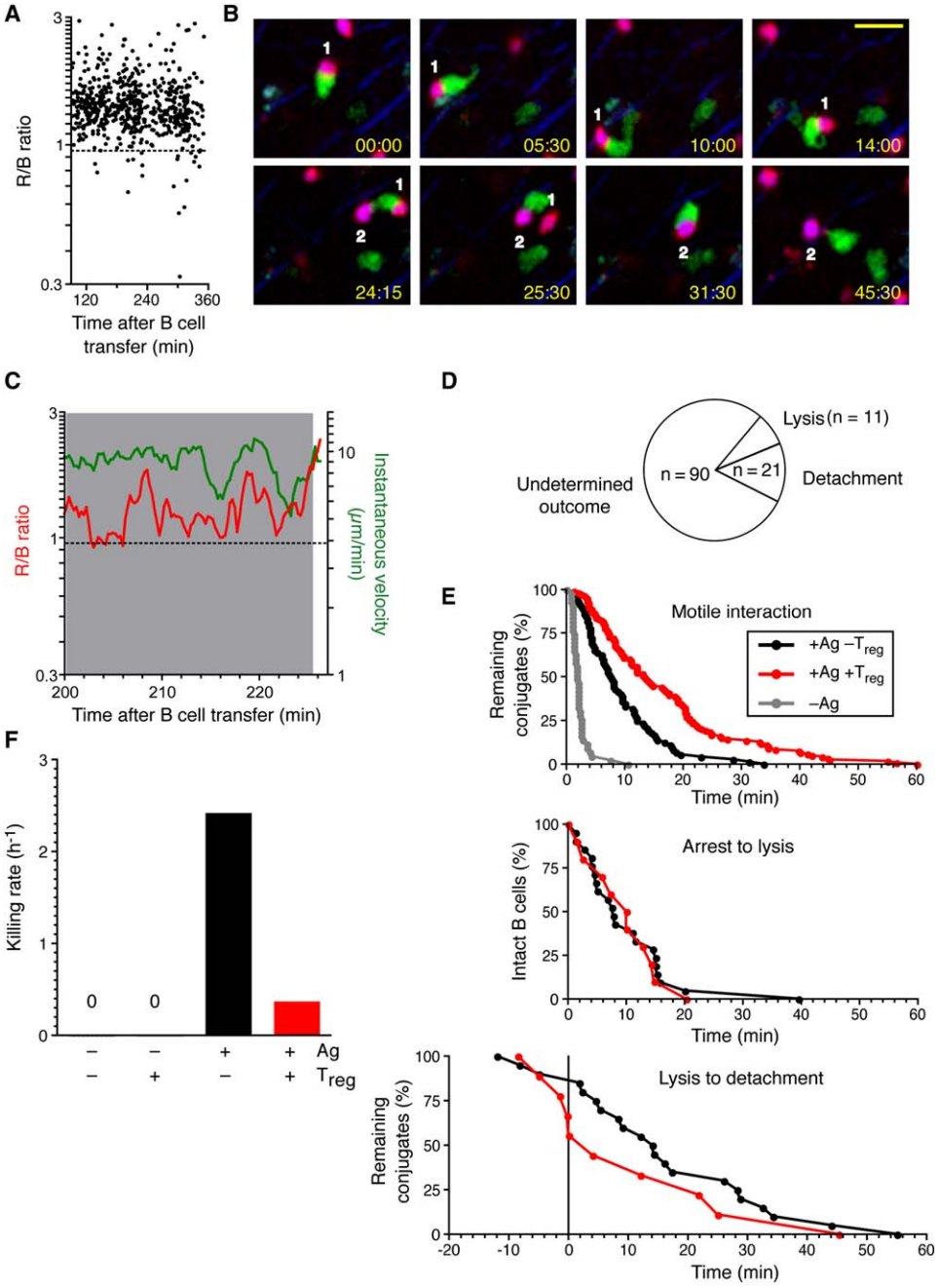


Figure 3. CTL-Mediated Induction of Motility Arrest and Lysis of B Cells Is Compromised in the Presence of $T_{reg}$ Cells

(A) R/B ratios of Ag-pulsed B cells imaged between 90 and 360 min after i.v. injection into mice containing regulated CTLs. Data are pooled from 11 recordings in 4 independent experiments.

(B) Representative micrographs showing a regulated CTL interacting with Ag-presenting B cells. After forming a motile conjugate with a B cell marked "1" for 25 min, the CTL engages with a second B cell ("2") and subsequently detaches from the first B cell, without inducing motility arrest or color change in either target cell. Scale bar equals 20 μm.

(C) Single-cell recording of time-averaged instantaneous migratory velocity (green line) and R/B ratio (red line) as indicators of viability of a B cell during an encounter with a regulated CTL (gray bar).

(D) Outcome of 122 distinct CTL-B cell interactions from four independent experiments. "Lysis" defines B cells with a R/B ratio that dropped below 0.95 after CTL interaction (see Experimental Procedures), "detachment" defines B cells that detached from CTLs and retained an R/B ratio above 0.95, and "undetermined outcome" defines CTL-B cell conjugates that left the recorded region before lysis or detachment could be observed.

(E) Cumulative frequencies of CTL-B cell conjugate persistence during each phase defined in Figure 2D. Top: persistence of motile conjugates from the moment of engagement to either motility arrest or early detachment. Results for interactions between CTLs and unpulsed B cells are shown in gray. Results with Ag-pulsed B cells are plotted for conjugates formed in the absence (black) or presence (red) of $T_{reg}$ cells. Middle: persistence of intact B cells (R/B ratio > 0.95) after motility arrest. Bottom: conjugate persistence from lysis to CTL detachment. All interactions for which the beginning and end of the interactive phase was observed were included. Motile interaction time was significantly increased in the presence of $T_{reg}$ cells ($p < 0.0001$), but times from arrest to lysis and from lysis to detachment were not significantly different.

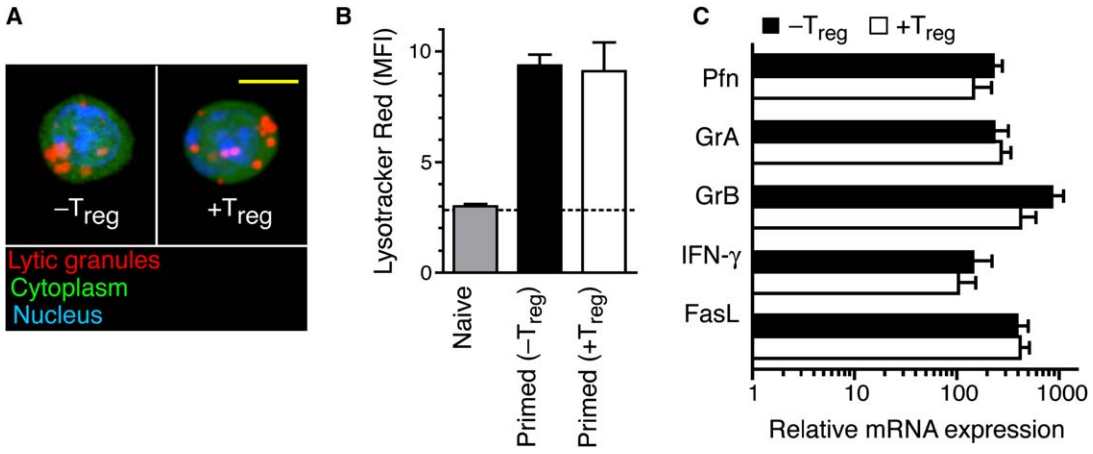


Figure 4. $T_{reg}$ Cells Do Not Compromise Effector Differentiation

(A) Fluorescent micrographs of nonregulated (left) and regulated CTL (right) purified from tumor-draining LNs at day 6 of the immune response. Cells were stained ex vivo for lytic granules (Lysotracker Red [Lyubchenko et al., 2001; Stinchcombe et al., 2001b]), nuclear DNA (Hoechst33342, blue), and cellular protein (CFSE, green) and imaged by confocal microscopy (scale bar equals 5 μm). Results are representative of three experiments.

(B) LN-derived regulated and nonregulated CTLs and naive $CD8^+$ T cells were assayed for lytic granule content by flow cytometry. Results are representative of two experiments with three mice per group. Mean and standard deviation are shown.

(C) Relative mRNA content (normalized to CD3ε) for various effector molecules in FACS-purified CTLs (1000 cells/sample). Nonregulated (black bars) and regulated (white bars) CTLs were isolated from day 7 tumor-draining LNs and analyzed by real-time PCR after reverse transcription. Results are representative of two independent experiments with three mice per group, each sample analyzed in triplicate. Mean and standard deviation are shown. Pfn, Perforin; GrA, GrB, Granzyme A, B; IFN-γ, Interferon-γ; FasL, Fas ligand.

the CTLs in tumor-draining LNs were highly cytotoxic, and the magnitude of their apparent desuppression correlated with the degree of $T_{reg}$ cell depletion (Figure 6B and Figure S4; data not shown). Thus, sustained CTL suppression requires the continuous presence of $T_{reg}$ cells.

### CTL Suppression Does Not Require Prolonged Physical Contacts with $T_{reg}$ Cells

Having determined that the continued physical presence of $T_{reg}$ cells in LNs after priming is required for CTL suppression, we set out to visualize how Ag-specific $T_{reg}$ cells behave and interact with CTLs in tumor-draining LNs. We adoptively transferred T cells from donor mice in which HA-specific $CD8^+$ T cells and $T_{reg}$ cells expressed red (DsRed) and green (EGFP) fluorescent tags, respectively. MP-IVM recordings during days 6 and 7 after tumor implantation showed that $T_{reg}$ cells as well as CTLs were highly motile and occupied primarily the deep paracortex and cortical ridge of tumor-draining LNs (Figures S2 and S5). Occasional CTLs and $T_{reg}$ cells could also be observed in B cell follicles. Unregulated CTL-B cell interactions were seen primarily in the T cell area where B cells enter LNs via high endothelial venules and are quickly eliminated by the resident CTLs. In the presence of $T_{reg}$ cells, CTL-B cell contacts were still initiated in the T cell zone, but some conjugates could be observed to enter follicles. In several instances, $T_{reg}$ cells and CTLs were recorded while undergoing cytokinesis, and a subset of cells (mostly CTLs) occasionally formed small clusters, presumably around endogenous Ag-presenting cells (Movies S4 and S6). However, nearly all physical encounters of $T_{reg}$ cells with CTLs lasted only a few minutes; tight conjugates of $T_{reg}$ cells and CTLs were rarely observed (Figures 7A and 7B and Movie S7), which is in line with another study that failed to detect prolonged $T_{reg}$ cell-$CD4^+$ T cell interactions during the priming phase in a model of autoimmune diabetes (Tang et al., 2006). In the few instances when $T_{reg}$ cells and CTLs showed prolonged colocalization, we did not detect a stable contact zone between them. Rather, they seemed to congregate around other nonfluorescent structures, possibly Ag-presenting cells.

### Discussion

$T_{reg}$ cells can inhibit immune responses in a variety of settings, but the mechanisms of suppression are still largely unclear. Here, we have described an imaging-based approach to examine the cellular functions that are altered in CTLs in the presence of activated $T_{reg}$ cells. We made use of a model in which regulated CTLs in tumor-draining LNs undergo normal clonal expansion but fail to exert cytotoxicity or to reject Ag-presenting tumors (Chen et al., 2005a). Unexpectedly, we found that regulated CTLs underwent essentially normal effector differentiation. Compared to nonregulated CTLs, the only detectable defect in regulated CTLs was a marked attenuation of Ag-triggered lytic granule release.

(F) The hourly killing rate of B cells by regulated and nonregulated CTLs was calculated as the ratio of the total number of observed killing events (defined by irreversible motility arrest) over the total cumulative duration of all recorded motile CTL-B cell conjugates from 3 to 6 experiments per group (that is ~100 min for CTL-$HA^-$ B cell conjugates, and ~700 min or ~2000 min for CTL-$HA^+$ B cell conjugates in the absence or presence of $T_{reg}$ cells, respectively).

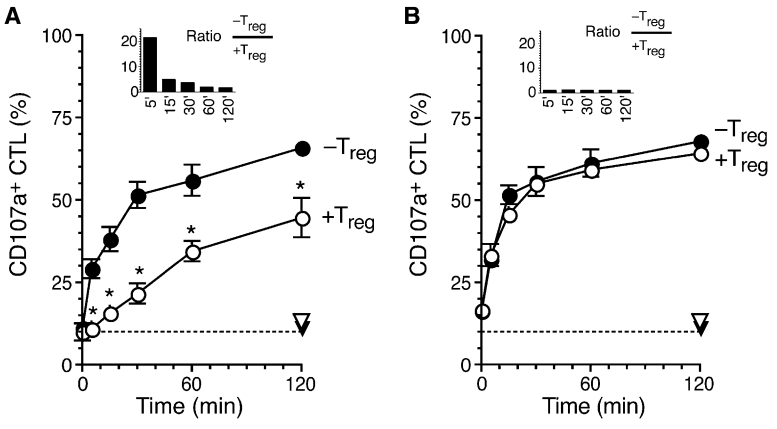


Figure 5. $T_{reg}$ Cells Selectively Interfere with CTL Granule Exocytosis in a TGF-β-Dependent Manner

(A) CTL degranulation as determined by cell-surface mobilization of the lysosomal marker CD107a (Betts et al., 2003) was measured by flow cytometry in CTL from tumor-draining LNs of mice that had also received $T_{reg}$ cells (empty symbols, $+T_{reg}$) or not (filled symbols, $-T_{reg}$). CTLs in single-cell suspensions of day 7 tumor-draining LNs were analyzed in the presence (circles) or absence (triangles) of HA-peptide. Dashed line indicates background staining. Total cellular CD107a was similar in both populations (Figure S3A). Insert shows the ratio of specific CD107a staining of nonregulated versus regulated CTLs at each time point. Results are pooled from seven independent experiments with three mice per group. Mean and standard deviation are shown.

(B) Degranulation of CTLs with a dominant-negative TGFβRII from day 7 tumor-draining LNs of mice transferred with $T_{reg}$ cells (empty symbols) or not (filled symbols). Results are pooled from three independent experiments with three mice per group. Mean and standard deviation are shown.

CTLs exert effector function by secreting cytokines, such as interferon-γ, and by cell contact-dependent cytotoxic lysis of targets that present a cognate Ag. The cellular processes governing cytotoxic killing have been extensively studied (reviewed in Lieberman, 2003), but an experimental approach that allows the characterization of CTL function on the single-cell level in vivo has not been described so far. By using MP-IVM, we now provide a space- and time-resolved analysis of how single CTLs kill their targets in situ. By using Ag-pulsed B cells as surrogate targets, we show that cytotoxic killing is a sequential process consisting of (1) rapid conjugate formation upon contact; (2) motile but stable and strictly monogamous interactions with target B cells, which always lead the way; (3) irreversible motility arrest of the conjugate; (4) loss of the target's structural integrity; and finally (5) detachment of the CTLs. The observation that motility arrest was always followed by loss of the victim's structural integrity suggests that permanent arrest represents the earliest indicator of irreversible cytotoxic damage. The cessation of motility might reflect a loss of cellular metabolism due to breakdown of mitochondrial function (Martinvalet et al., 2005). The subsequent loss of structural integrity was probably triggered by direct and indirect actions of granzymes on the nuclear envelope, chromatin, and other essential structural elements (Lieberman, 2003).

Strikingly, similar to what has been described for activated $CD4^+$ T cells providing help to B cells (Okada et al., 2005), Ag recognition triggered the immediate formation of stable contacts between CTLs and Ag-presenting B cells. By contrast, when naive T cells encounter

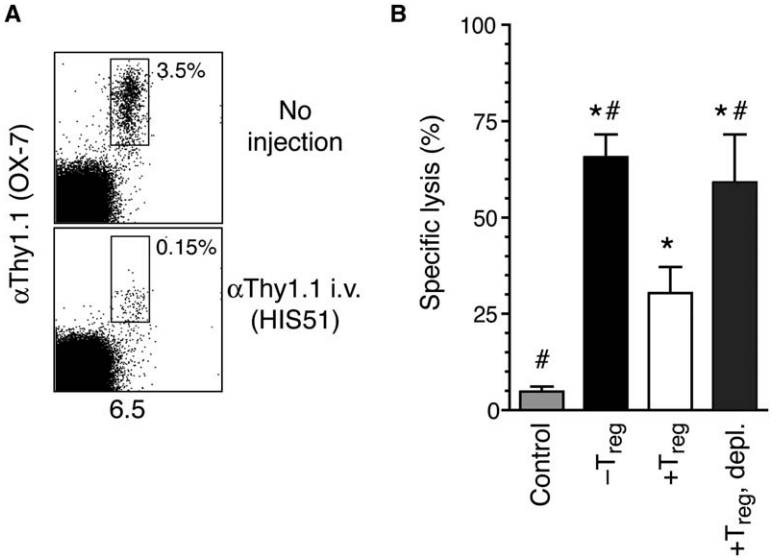


Figure 6. $T_{reg}$ Cell-Induced CTL Killing Inefficiency Is Reversible In Vivo upon Removal of $T_{reg}$ Cells

(A) Content of $Thy1.1^+$ adoptively transferred $T_{reg}$ cells in LNs of $Thy1.2^+$ control mice after injection (bottom) or not (top) of 400 μg Thy1.1 mAb HIS51 on day 5 and 6 of the immune response. $T_{reg}$ cell depletion was assessed on day 8 by the clonotypic mAb 6.5 and Thy1.1 mAb OX-7.

(B) In vivo killing activity in tumor-draining LNs was measured on day 8 as described in Experimental Procedures. Compared to nonregulated CTLs ($-T_{reg}$), regulated CTLs ($+T_{reg}$) showed reduced cytotoxicity, but they acquired potent cytotoxic activity after $T_{reg}$ cell depletion ($+T_{reg}$, depleted). Mean and standard deviation from three mice per group are shown. #$p < 0.05$ versus $+T_{reg}$; *$p < 0.05$ versus control (tumor-draining LN without HA-specific CTLs).

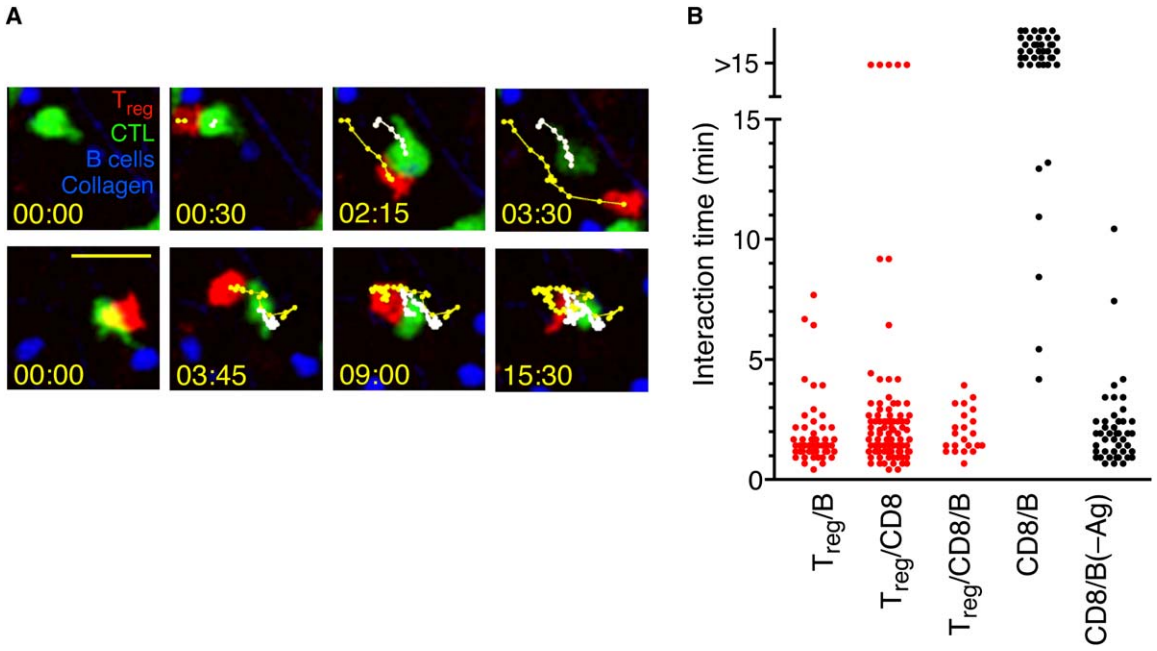


Figure 7. $T_{reg}$ Cell-Mediated Suppression Does Not Require Prolonged $T_{reg}$ Cell/CTL Contact

(A) MP-IVM micrographs highlighting the interactive behavior of ds-Red$^+$ $T_{reg}$ cells (red) and EGFP$^+$ CTLs (green) in tumor-draining LN (day 6). Upper panels show a brief contact; lower panels show a rare, longer-lasting colocalization. Ag-pulsed B cells and collagen fibers are shown in blue. Yellow and white dots represent $T_{reg}$ cell and CTL tracks, respectively. These micrographs are from Movie S7. Time passed after capturing the first image (left) is shown in minutes and seconds. Scale bar equals 20 μm. Similar results were obtained with EGFP$^+$ $T_{reg}$ cells and ds-Red$^+$ CTLs (not shown).

(B) Duration of contacts of $T_{reg}$ cells with Ag-pulsed B cells, CTLs, and CTL-B cells conjugates (red symbols) and of regulated CTLs with Ag-pulsed or unpulsed B cells in the same recordings (two independent experiments).

Ag-presenting DCs, they undergo a prolonged phase of transient contacts before engaging in tight interactions (Hugues et al., 2004; Mempel et al., 2004; Miller et al., 2004; Tang et al., 2006). This behavioral difference could be due to the distinct character of the Ag-presenting cells (mature DC versus B cell) and/or differential responsiveness to Ag of naive versus primed effector T cells. In vitro, Ag-presenting B cells support immediate firm adhesion of T cells, whereas DCs promote only transient contact (Gunzer et al., 2004). Activated T cells, on the other hand, are known to respond faster to Ag recognition than naive T cells. The rules that govern this decision-making process in vivo remain to be defined.

In vitro studies have shown that $T_{reg}$ cells prohibit activation-induced proliferation of effector T cells (Shevach, 2002). There is also evidence that suppression of proliferation is a relevant mechanism of regulation in certain in vivo settings (Tang et al., 2006). However, other in vivo studies provide evidence that even under conditions that allow expansion of effector cells, $T_{reg}$ cells can attenuate T cell-mediated immune responses, e.g., in transplantation tolerance (Lin et al., 2002); chronic viral infection (Dittmer et al., 2004); and in tumor responses in both mice (Chen et al., 2005a; Thomas and Massague, 2005) and humans (Curiel et al., 2004; Sato et al., 2005; Zippelius et al., 2004).

Our MP-IVM recordings show that regulated CTLs occupy the same LN microenvironment and display similar motility as unregulated CTLs. Also, regulated CTLs retain the ability to form Ag-dependent motile conjugates, but they are strikingly inefficient at lysing Ag-presenting targets. This suggests a disconnection between the signaling events that trigger CTL adhesion to the target cell and other Ag-triggered cellular functions required for target cell killing. Indeed, $T_{reg}$ cell-mediated impairment of CTL function has been suggested previously in a setting of chronic viral infection (Dittmer et al., 2004). More recently, two studies have reported deficiencies in lytic effector molecules in CTLs in mouse models of chronic viral infection (Zelinskyy et al., 2005) and antitumor response (Thomas and Massague, 2005). The latter study also demonstrated that the presence of TGF-β during in vitro activation of CD8$^+$ T cells leads to diminished content in perforin, granzymes A and B, Fas ligand, and IFN-γ. In our model, the analysis of mRNA expression of these effector molecules did not detect compromised differentiation of regulated CTLs. We also did not find a substantial reduction in granzyme B protein, but we can not exclude $T_{reg}$ cell-induced changes in content of other effector molecules due to posttranscriptional effects, or effects that may be apparent only at different time points of the immune response. Nevertheless, our findings indicate that CTL differentiation is minimally affected by $T_{reg}$ cells. The only striking difference between regulated and nonregulated CTLs was the inability of the former to degranulate. Earlier work has shown that genetic defects in granule secretion (e.g., due to Rab27a deficiency) cause a profound inability of CTLs to kill target cells (Stinchcombe et al., 2001a). Thus, the $T_{reg}$ cell-induced deficiency in degranulation is likely to account for the poor cytotoxic activity of regulated CTLs.

Differential regulation of granule polarization and release has also been described for NK cells (Bryceson et al., 2005), which, unlike T cells, express cytolytic molecules constitutively and are triggered by different receptors to degranulate (Lieberman, 2003). However, it remains to be determined whether and to what extent the control mechanisms of NK degranulation are evoked in regulated CTLs.

One clue for a potential mechanism by which degranulation may be regulated is suggested by observations in tumor-infiltrating lymphocytes (TILs) (Koneru et al., 2005; Radoja et al., 2001). Frey and colleagues found that freshly isolated TILs that were unable to lyse target cells contained normal amounts of perforin and granzyme B but could not polarize their MTOC to release their granules (Radoja et al., 2001). Upon isolation and culture, the cells recovered their degranulation capacity and cytotoxicity within 12 hr. This recovery depended on proteosomal function and was paralleled by recovery of MTOC and granule polarization, indicating an active mechanism of inhibition whose reversal required protein degradation (Radoja et al., 2001). The degranulation defect in freshly isolated TILs was attributed to dysfunctional proximal TCR signaling (Koneru et al., 2005). In the present model, the response of regulated LN-resident CTLs to cognate Ag was indistinguishable from that of nonregulated CTLs with regard to their proliferation, activation-induced IFN-$\gamma$ production, and Ag-dependent conjugate formation with target cells. Thus, it is unlikely that TCR signaling was globally compromised in the regulated CTLs observed here. However, it is possible that $T_{reg}$ cell-mediated suppression induces more subtle changes in signaling cascades triggered by TCR engagement in CTLs, which might account for the defective degranulation. Of note, the negative regulator of TCR signaling, PD-1, has been shown to be expressed on CTLs in chronic viral infection (Barber et al., 2006). It will be interesting to determine whether $T_{reg}$ cells induce PD-1 expression on CTLs, attenuating TCR signaling upon encounter with PD-L1-expressing target cells. PD-L1 is expressed on several nonhematopoetic tissues, including a variety of tumors (Latchman et al., 2004).

Suppression of cytotoxicity was reversible if $T_{reg}$ cells are depleted after CTL priming, indicating that $T_{reg}$ cells must continuously "remind" CTLs to maintain suppression. This rapid (within less than 3 days) reversibility of suppression could be beneficial in settings where simultaneous stimulation of $T_{reg}$ cells and $CD8^+$ T cells in lymphoid organs would allow the generation of large numbers of effector cells while preventing the premature killing of Ag-presenting cells. Once the CTLs have returned to the circulation, they may quickly unleash their full cytotoxic force upon entering a peripheral site of inflammation where $T_{reg}$ cells may either not have access or their function is antagonized. For example, inflammatory and pathogen-derived signals can release CTLs from the suppressive effect of $T_{reg}$ cells (Pasare and Medzhitov, 2003, 2004; Peng et al., 2005; Waldmann et al., 2004). In this scenario, $T_{reg}$ cell activity in LNs might paradoxically boost immune responses to pathogens by promoting CTL priming in lymphoid tissues and by focusing their effector activity to peripheral sites of pathogen invasion.

In tissue-culture experiments, cell-cell contact between $T_{reg}$ cells and regulated T cells seems to be required for suppression, while cytokines are dispensable (Shevach, 2002). However, in vivo studies imply an important role for secreted mediators, especially TGF-$\beta$ (Gorelik and Flavell, 2002). Since we could reverse suppression of CTLs by depletion of $T_{reg}$ cells after day 5 of the immune response, we conclude that regulation is still ongoing and required at this late time point. However, while CTLs formed numerous long-lasting motile conjugates with peptide-pulsed B cells, the migrating $T_{reg}$ cells in the same field of view collided only briefly with B cells, CTLs, or B cell-CTL conjugates; long-lived ternary aggregates between B cells, CTLs, and $T_{reg}$ cells were absent. Nevertheless, B cells were rarely killed in this setting, indicating that CTL suppression does not require prolonged $T_{reg}$ cell contact with either the effector cells or their targets. It is possible that contact-dependent suppressive signals (e.g., through the CD28-CTLA-4 pathway [Sakaguchi, 2004]) are exchanged during the brief collisions between activated $T_{reg}$ cells and CTLs. However, our results suggest that $T_{reg}$ cells exert their activity on CTLs, at least in part, by inducing a local milieu that is rich in TGF-$\beta$ and probably other suppressive factors. Such a regulatory environment prohibits CTL degranulation and, thus, cytolysis, independent of effects during T cell priming.

A recent multiphoton microscopy study on $T_{reg}$ cell function in excised pancreatic LNs of diabetes-prone mice reported that $T_{reg}$ cells undergo tight interactions only with islet-Ag presenting DCs, but not with diabetogenic $CD4^+$ effector cells (Tang et al., 2006). This is consistent with the present finding that $T_{reg}$ cells in tumor-draining LNs do not engage in stable contacts with CTLs, although DCs (or other tumor Ag-presenting cells) were not visualized here. In the autoimmune diabetes model, the presence of $T_{reg}$ cells impaired proliferation and expansion of diabetogenic $CD4^+$ T cells, while CTL proliferation was not affected in our tumor model. However, inhibition of proliferation of diabetogenic T cells was observed only when islet Ag-specific $T_{reg}$ cells were transferred 2 days earlier, thus allowing the $T_{reg}$ cells sufficient time to become activated and, presumably, to alter DC function (Tang et al., 2006). Simultaneous transfer of $T_{reg}$ cells and effector cell precursors (similar to the protocol used here) did not block effector cell proliferation (Tang et al., 2006), even though the delayed transfer of $T_{reg}$ cells is still sufficient to prohibit disease in diabetes-prone mice (Tang et al., 2004). Indeed, another study found that the control of diabetogenic effector cells by naturally occurring endogenous $T_{reg}$ cells does not affect the expansion or differentiation of effector cells in pancreatic LNs (Chen et al., 2005b). In this setting, effector cell precursors and $T_{reg}$ cells are likely to encounter islet Ags at the same time (Turley et al., 2003). Although these studies investigated the suppression of autoreactive $CD4^+$ T cells, a striking commonality with our observations of foreign Ag-specific CTLs is that simultaneous activation of $T_{reg}$ cells leads to effector suppression without impairment of effector expansion at the priming site.

These diverse observations emphasize that $T_{reg}$ cells can suppress immune responses at multiple levels and that distinct or even contradictory mechanisms and

consequences may predominate the experimental readout under different circumstances. In our model, the initially small number of LN-resident $T_{reg}$ cells probably first need to be activated and clonally expand before they can confer suppressive signals to CTLs. Thus, regulation may only take effect late after CTL priming and effector differentiation.

In conclusion, our results show that $T_{reg}$ cells can selectively interfere with the release of cytolytic granules by CTLs in a reversible and TGF-β-dependent manner. Thereby, $T_{reg}$ cells attenuate CTL cytotoxicity without detectably affecting priming or differentiation. This finding has implications for the design of therapeutic strategies that rely on modulating ongoing immune responses. Our findings support the notion that local or systemic interference with suppressor pathways of CTL activity, e.g., with cytokines (Sakaguchi et al., 1995; Shevach, 2002) or Toll-like receptor agonists (Pasare and Medzhitov, 2003, 2004; Peng et al., 2005) or $T_{reg}$ cell depletion (Yang et al., 2004), may be effective in the case of tumor therapy, where immunity is desired. Conversely, promoting suppression by targeting pathways that enhance or mimic $T_{reg}$ cell activity may be clinically useful to induce or maintain tolerance in the context of allotransplantation or autoimmunity.

## Experimental Procedures

### Mice

DPE-GFP and T-Red transgenic mice were generated by means of modifications of a previously described construct (Manjunath et al., 1999), which induce uniform and selective expression of EGFP or ds-RedII, respectively, in T cells, including effector cells. DPE-GFP × TCR-CL4 × Rag-$2^{-/-}$ mice were generated by crossing the DPE-GFP strain to TCR-CL4 × Rag-$2^{-/-}$ mice, which express a transgenic TCR specific for H-$2K^d$/$HA_{512-520}$ (Morgan et al., 1996). T-Red × pgk-HA × TCR-HA mice were obtained by crossing T-Red mice to pgk-HA × TCR-HA mice expressing influenza-HA under the control of the phosphoglycerate kinase promotor and a transgenic TCR specific for I-$E^d$/$HA_{107-119}$ (Chen et al., 2005a). T-Red × TCR-CL4 × Rag-$2^{-/-}$ and DPE-GFP × pgk-HA × TCR-HA mice were generated accordingly. TCR-CL4 × Rag-$2^{-/-}$ mice were also crossed to dnTGFβRII transgenic mice, a generous gift from Dr. Richard Flavell (Gorelik and Flavell, 2000). Thy1.$1^+$ BALB/c mice were obtained from Dr. Paul Allen and used as such or crossed to the pgk-HA × TCR-HA mice. Thy1.$2^+$ BALB/c mice were obtained from Jackson Laboratories. All mice were housed in specific pathogen-free conditions in compliance with guidelines set by the Sub-Committee on Animal Research Care at the Massachusetts General Hospital.

### Cells

HA-specific $CD8^+$ T cells and HA-specific $CD4^+$ $CD25^+$ regulatory T cells were purified from DPE-GFP TCR-CL4 × Rag-$2^{-/-}$ or TCR-CL4 × Rag-$2^{-/-}$ mice and T-Red × pgk-HA × TCR-HA or pgk-HA × TCR-HA mice, respectively, as described (Chen et al., 2005a). B cells from LNs and spleens of Thy1.$1^+$ mice were purified by CD43-negative immunomagnetic cell sorting (Miltenyi Biotec). Purity was typically greater than 95%. The tumor cell line CT44 was generated by stably transfecting CT26 cells (ATCC, Manassas, VA) with a fusion protein of influenza haemagglutinin and EGFP (Klein et al., 2003b).

### mAbs and Flow Cytometry

TCR-HA mAb (clone 6.5) was grown and purified according to standard procedures. All other mAbs were from BD Pharmingen. Phenotypic characterization of T and B cells was performed on a FACSCalibur (Becton Dickinson).

### Ex Vivo Degranulation Assay

CTL granule exocytosis was measured as mobilization of the lysosomal marker CD107a (Lamp-1) to the cell surface as described (Betts et al., 2003). In brief, tumor-draining LNs containing locally primed HA-specific CTLs and either HA-specific $T_{reg}$ cells or not were harvested on day 6 or 7. $HA_{512-520}$, $HA_{107-119}$, and FITC-conjugated CD107a mAb were then added to LN cell suspensions on ice and aliquots taken at various time points after rapidly warming to 37°C to trigger Ag-induced degranulation and detect CD107a molecules subsequently exposed at the cell surface. After all aliquots had been sampled, cell suspensions were stained for 20 min on ice for the congenic marker Thy1.2 and for CD8α to identify HA-specific CTLs as well as for CD107a to adjust unspecific background staining between all samples and analyzed by flow cytometry.

### In Vitro Imaging of CTLs

To assess secretory granule content, CTLs were sorted from LNs and stained with 50 nM Lysotracker Red (Molecular Probes) (Lyubchenko et al., 2001; Stinchcombe et al., 2001b) for 2 hr and either analyzed by flow cytometry or additionally stained with 2.5 μM Hoechst33342 and 5 μM carboxyfluoresceine diacetate, succinimidyl ester (CFSE, Molecular Probes), and adhered to poly-l-lysine-coated cover slips and imaged by confocal microscopy.

### Real-Time RT-PCR

Aliquots of $10^3$ CTLs were sorted from LNs on day 6, and mRNA levels for various genes were determined as described (Peixoto et al., 2004). Expression levels were normalized for CD3ε mRNA, since CD3ε protein was expressed on the cell surface at similar levels and CD3ε message levels did not vary between regulated and unregulated CTLs in the same experiment.

### In Vivo $T_{reg}$ Cell Depletion

Thy1.$2^+$ BALB/c mice received intravenous injections of $10^5$ HA-specific Thy1.$2^+$ $CD8^+$ T cells and $10^5$ HA-specific Thy1.$1^+$ $CD4^+$ $CD25^+$ $T_{reg}$ cells, followed by implantation of HA-expressing tumors into the footpad. Thy1.$1^+$ $T_{reg}$ cells were depleted from Thy1.$2^+$ mice containing Thy1.$2^+$ CTLs by intravenous injections of anti-Thy1.1 mAb (HIS51, 400 μg/day) on day 5 and 6 of the immune response.

### In Vivo Killing Assay

$HA_{512-520}$-pulsed and unpulsed B cells were incubated with 0.2 μM ($CFSE^{low}$) and 2 μM CFSE ($CFSE^{high}$) for 15 min in PBS-1% FBS, respectively, and $2 \times 10^7$ total cells injected intravenously at a 1:1 ratio into tumor-bearing recipients that had either not received T cells or received HA-specific $CD8^+$ T cells together with or without $T_{reg}$ cells ("exp"). After 6 hr, the frequency of pulsed and unpulsed B cells was determined in tumor-draining LNs by FACS. Injection of mice that had received neither tumors nor T cells served to control for variability in B cell input ratio and unspecific B cell death ("ctrl"). Percent specific lysis was calculated as follows: $(1 - CFSE^{low(exp)}/CFSE^{high(exp)} / CFSE^{low(ctrl)}/CFSE^{high(ctrl)}) \times 100$ (%).

### Intravital Multiphoton Microscopy

B cells were pulsed with $HA_{512-520}$ (Biosource) or left unpulsed, labeled for 30 min at 37°C with 2.5 μM Hoechst33342 (Molecular Probes), and then washed and labeled for 15 min at 37°C with 20 μM 5-(and 6-)-(((4-chloromethyl) benzoyl) amino) tetramethylrhodamine (CMTMR; Molecular Probes). $2 \times 10^7$ B cells in 100 μl RPMI were injected i.v. into tumor-bearing mice. At various time points during the following 15 hr, mice were anesthetized and the tumor-draining popLN was prepared microsurgically for MP-IVM on a BioRad 2100MP system as described (Mempel et al., 2004). For multiphoton excitation and second harmonic generation, a MaiTai Ti:sapphire laser (Spectra-Physics) was tuned between 900 and 960 nm to balance excitation of the various fluorescent probes used. For four-dimensional analysis of cell migration, stacks of 11 square x-y sections with 4 μm z spacing were acquired every 15 s with electronic zooming up to 4× to provide image volumes 40 μm in depth and between 154 and 618 μm in width. Emitted light and second harmonic signals were detected through 450/80 nm, 525/50 nm, and 630/120 nm band-pass filters with nondescanned detectors to generate three-color images. Sequences of image stacks were transformed into volume-rendered, four-dimensional

time-lapse movies with Volocity software (Improvision). Velocity measurements were done by semiautomated cell tracking with Volocity (Improvision) and computational analysis by Matlab (Mathworks). Red and blue mean fluorescence pixel intensities of B cells rendered in maximum intensity projections were measured on single cells with Openlab (Improvision).

Parameters of cell motility were determined as described previously (Sumen et al., 2004). To display the 3D velocity of individual migrating B cells, velocity tracks were smoothed by calculating the time-averaged instantaneous velocity, which represents the mean of 21 individual instantaneous velocity measurements derived for each time point from the 10 preceding and the 10 subsequent determinations. This parameter was also used to discern motile from immotile cells via a reference population of 40 viable B cells, 95% of which had a mean track velocity >3.9 μm/min. B cells whose time-averaged velocity was permanently below this 5$^{th}$ percentile cutoff were defined as immotile. The fact that the measured velocity of most immotile cells was >0 μm/min is due to movement or drift of the preparation and passive displacement of dead cells colliding with migrating viable cells.

In each individual MP-IVM recording (n = 22 recordings in 9 mice), laser power, excitiation wavelength, and gain settings were adjusted for optimally balanced signal intensities in all color channels at a given imaging depth. Due to case-by-case differences in these acquisition parameters, the mean R/B ratios of viable motile B cells that did not interact with CTL were somewhat variable, ranging from 0.87 to 2.93 (mean ± SD: 1.43 ± 0.42). To allow a side-by-side comparison of R/B ratios from different recordings, we calculated the average R/B ratio of viable cells from all 22 recordings, $\bar{R/B}_{global}$. We then determined the correction factor $c$ for each individual recording according to $c = \bar{R/B}_{global} / \bar{R/B}_{exp}$, where $\bar{R/B}_{exp}$ is the mean R/B ratio of all motile noninteracting B cells within that recording. This correction factor was then applied to the measured R/B ratio of each individual B cell (motile or immotile), $R/B_{cell}$, in the same recording to obtain the corrected R/B ratio: $R/B_{corrected} = R/B_{cell} \times c$. All results referred to as "R/B ratio" in figures and text represent $R/B_{corrected}$. Individual B cells were considered to be structurally damaged when their $R/B_{corrected}$ dropped below 0.95, which represents the 5$^{th}$ percentile of $R/B_{corrected}$ values from a reference population consisting of all 470 viable B cells analyzed in this study.

### Statistical Analysis

Unless indicated otherwise, data are expressed as mean ± SEM. Differences between groups were tested via an unpaired, two-tailed t test.

### Supplemental Data

Supplemental Data include six figures and seven movies and can be found with this article online at http://www.immunity.com/cgi/content/full/25/1/129/DC1/.

### Acknowledgments

We thank Drs. Richard Flavell and Leonid Gorelik for dnTGFbRII mice, Dr. Paul Allen for Thy1.1$^+$ BALB/c mice, Dr. Karsten Kretschmer for Thy1.1$^+$ pgk-HA × TCR-HA mice, Andrew Intlekofer and Steve Reiner for assistance with PCR, Antonio Peixoto for advice with PCR, Fay Magnusson, Dina Laznik, and Linda Coulson for assistance, and Sarah Henrickson and Tim Buschman for software programming. T.R.M. is supported by a NIH training grant (T32-HL-066987-04) and M.J.P. by the Human Frontier Science Program Organization (LT00369/2003). This work was supported in part by NIH grants RO-AI-061663, RO1-HL54936, and PO1-HL56949 (to U.H.v.A.); RO1-CA96978 and RO1-CA104547 (to K.K); P50-CA-86355 and R24-CA92782 (to R.W.); and R37 AI53102 (to H.v.B); by the Claudia Adams Barr Program in Cancer Research (to K.K.); and by the Dana Foundation Immuno-Imaging Program (to U.H.v.A.). The authors declare that they have no competing financial interests.

Received: February 2, 2006
Revised: March 20, 2006
Accepted: April 14, 2006
Published: July 25, 2006

### References

Barber, D.L., Wherry, E.J., Masopust, D., Zhu, B., Allison, J.P., Sharpe, A.H., Freeman, G.J., and Ahmed, R. (2006). Restoring function in exhausted CD8 T cells during chronic viral infection. Nature *439*, 682–687.

Betts, M.R., Brenchley, J.M., Price, D.A., De Rosa, S.C., Douek, D.C., Roederer, M., and Koup, R.A. (2003). Sensitive and viable identification of antigen-specific CD8+ T cells by a flow cytometric assay for degranulation. J. Immunol. Methods *281*, 65–78.

Bryceson, Y.T., March, M.E., Barber, D.F., Ljunggren, H.G., and Long, E.O. (2005). Cytolytic granule polarization and degranulation controlled by different receptors in resting NK cells. J. Exp. Med. *202*, 1001–1012.

Chen, M.L., Pittet, M.J., Gorelik, L., Flavell, R.A., Weissleder, R., von Boehmer, H., and Khazaie, K. (2005a). Regulatory T cells suppress tumor-specific CD8 T cell cytotoxicity through TGF-beta signals in vivo. Proc. Natl. Acad. Sci. USA *102*, 419–424.

Chen, Z., Herman, A.E., Matos, M., Mathis, D., and Benoist, C. (2005b). Where CD4+CD25+ T reg cells impinge on autoimmune diabetes. J. Exp. Med. *202*, 1387–1397.

Curiel, T.J., Coukos, G., Zou, L., Alvarez, X., Cheng, P., Mottram, P., Evdemon-Hogan, M., Conejo-Garcia, J.R., Zhang, L., Burow, M., et al. (2004). Specific recruitment of regulatory T cells in ovarian carcinoma fosters immune privilege and predicts reduced survival. Nat. Med. *10*, 942–949.

Dittmer, U., He, H., Messer, R.J., Schimmer, S., Olbrich, A.R., Ohlen, C., Greenberg, P.D., Stromnes, I.M., Iwashiro, M., Sakaguchi, S., et al. (2004). Functional impairment of CD8(+) T cells by regulatory T cells during persistent retroviral infection. Immunity *20*, 293–303.

Dustin, M.L., Bromley, S.K., Zhengyan, K., Peterson, D.A., and Unanue, E.R. (1997). Antigen receptor engagement delivers a stop signal to migrating T lymphocytes. Proc. Natl. Acad. Sci. USA *94*, 3909–3913.

Gorelik, L., and Flavell, R.A. (2000). Abrogation of TGFbeta signaling in T cells leads to spontaneous T cell differentiation and autoimmune disease. Immunity *12*, 171–181.

Gorelik, L., and Flavell, R.A. (2002). Transforming growth factor-beta in T-cell biology. Nat. Rev. Immunol. *2*, 46–53.

Gunzer, M., Weishaupt, C., Hillmer, A., Basoglu, Y., Friedl, P., Dittmar, K.E., Kolanus, W., Varga, G., and Grabbe, S. (2004). A spectrum of biophysical interaction modes between T cells and different antigen-presenting cells during priming in 3-D collagen and in vivo. Blood *104*, 2801–2809.

Hugues, S., Fetler, L., Bonifaz, L., Helft, J., Amblard, F., and Amigorena, S. (2004). Distinct T cell dynamics in lymph nodes during the induction of tolerance and immunity. Nat. Immunol. *5*, 1235–1242.

Klein, L., Khazaie, K., and von Boehmer, H. (2003a). In vivo dynamics of antigen-specific regulatory T cells not predicted from behavior in vitro. Proc. Natl. Acad. Sci. USA *100*, 8886–8891.

Klein, L., Trautman, L., Psarras, S., Schnell, S., Siermann, A., Liblau, R., von Boehmer, H., and Khazaie, K. (2003b). Visualizing the course of antigen-specific CD8 and CD4 T cell responses to a growing tumor. Eur. J. Immunol. *33*, 806–814.

Kohler, M., Zaitsev, S.V., Zaitseva, I.I., Leibiger, B., Leibiger, I.B., Turunen, M., Kapelioukh, I.L., Bakkman, L., Appelskog, I.B., de Monvel, J.B., et al. (2003). On-line monitoring of apoptosis in insulin-secreting cells. Diabetes *52*, 2943–2950.

Koneru, M., Schaer, D., Monu, N., Ayala, A., and Frey, A.B. (2005). Defective proximal TCR signaling inhibits CD8+ tumor-infiltrating lymphocyte lytic function. J. Immunol. *174*, 1830–1840.

Kullberg, M.C., Hay, V., Cheever, A.W., Mamura, M., Sher, A., Letterio, J.J., Shevach, E.M., and Piccirillo, C.A. (2005). TGF-beta1 production by CD4(+)CD25(+) regulatory T cells is not essential for suppression of intestinal inflammation. Eur. J. Immunol. *35*, 2886–2895.

Latchman, Y.E., Liang, S.C., Wu, Y., Chernova, T., Sobel, R.A., Klemm, M., Kuchroo, V.K., Freeman, G.J., and Sharpe, A.H. (2004). PD-L1-deficient mice show that PD-L1 on T cells, antigen-presenting

cells, and host tissues negatively regulates T cells. Proc. Natl. Acad. Sci. USA *101*, 10691–10696.

Lieberman, J. (2003). The ABCs of granule-mediated cytotoxicity: new weapons in the arsenal. Nat. Rev. Immunol. *3*, 361–370.

Lin, C.Y., Graca, L., Cobbold, S.P., and Waldmann, H. (2002). Dominant transplantation tolerance impairs CD8+ T cell function but not expansion. Nat. Immunol. *3*, 1208–1213.

Lyubchenko, T.A., Wurth, G.A., and Zweifach, A. (2001). Role of calcium influx in cytotoxic T lymphocyte lytic granule exocytosis during target cell killing. Immunity *15*, 847–859.

Manjunath, N., Shankar, P., Stockton, B., Dubey, P.D., Lieberman, J., and von Andrian, U.H. (1999). A transgenic mouse model to analyze CD8(+) effector T cell differentiation in vivo. Proc. Natl. Acad. Sci. USA *96*, 13932–13937.

Martinvalet, D., Zhu, P., and Lieberman, J. (2005). Granzyme A induces caspase-independent mitochondrial damage, a required first step for apoptosis. Immunity *22*, 355–370.

Mempel, T.R., Henrickson, S.E., and von Andrian, U.H. (2004). T cell priming by dendritic cells in lymph nodes occurs in three distinct phases. Nature *427*, 154–159.

Miller, M.J., Safrina, O., Parker, I., and Cahalan, M.D. (2004). Imaging the single cell dynamics of CD4+ T cell activation by dendritic cells in lymph nodes. J. Exp. Med. *200*, 847–856.

Morgan, D.J., Liblau, R., Scott, B., Fleck, S., McDevitt, H.O., Sarvetnick, N., Lo, D., and Sherman, L.A. (1996). CD8(+) T cell-mediated spontaneous diabetes in neonatal mice. J. Immunol. *157*, 978–983.

Okada, T., Miller, M.J., Parker, I., Krummel, M.F., Neighbors, M., Hartley, S.B., O'Garra, A., Cahalan, M.D., and Cyster, J.G. (2005). Antigen-engaged B cells undergo chemotaxis toward the T zone and form motile conjugates with helper T cells. PLoS Biol. *3*, e150. 10.1371/journal.pbio.0030150.

Pasare, C., and Medzhitov, R. (2003). Toll pathway-dependent blockade of CD4+CD25+ T cell-mediated suppression by dendritic cells. Science *299*, 1033–1036.

Pasare, C., and Medzhitov, R. (2004). Toll-dependent control mechanisms of CD4 T cell activation. Immunity *21*, 733–741.

Pearce, E.L., Mullen, A.C., Martins, G.A., Krawczyk, C.M., Hutchins, A.S., Zediak, V.P., Banica, M., DiCioccio, C.B., Gross, D.A., Mao, C.A., et al. (2003). Control of effector CD8+ T cell function by the transcription factor Eomesodermin. Science *302*, 1041–1043.

Peixoto, A., Monteiro, M., Rocha, B., and Veiga-Fernandes, H. (2004). Quantification of multiple gene expression in individual cells. Genome Res. *14*, 1938–1947.

Peng, G., Guo, Z., Kiniwa, Y., Voo, K.S., Peng, W., Fu, T., Wang, D.Y., Li, Y., Wang, H.Y., and Wang, R.F. (2005). Toll-like receptor 8-mediated reversal of CD4+ regulatory T cell function. Science *309*, 1380–1384.

Radoja, S., Saio, M., Schaer, D., Koneru, M., Vukmanovic, S., and Frey, A.B. (2001). CD8(+) tumor-infiltrating T cells are deficient in perforin-mediated cytolytic activity due to defective microtubule-organizing center mobilization and lytic granule exocytosis. J. Immunol. *167*, 5042–5051.

Sakaguchi, S. (2004). Naturally arising CD4+ regulatory t cells for immunologic self-tolerance and negative control of immune responses. Annu. Rev. Immunol. *22*, 531–562.

Sakaguchi, S., Sakaguchi, N., Asano, M., Itoh, M., and Toda, M. (1995). Immunologic self-tolerance maintained by activated T cells expressing IL-2 receptor alpha-chains (CD25). Breakdown of a single mechanism of self-tolerance causes various autoimmune diseases. J. Immunol. *155*, 1151–1164.

Sato, E., Olson, S.H., Ahn, J., Bundy, B., Nishikawa, H., Qian, F., Jungbluth, A.A., Frosina, D., Gnjatic, S., Ambrosone, C., et al. (2005). Intraepithelial CD8+ tumor-infiltrating lymphocytes and a high CD8+/regulatory T cell ratio are associated with favorable prognosis in ovarian cancer. Proc. Natl. Acad. Sci. USA *102*, 18538–18543.

Shevach, E.M. (2002). CD4+ CD25+ suppressor T cells: more questions than answers. Nat. Rev. Immunol. *2*, 389–400.

Stinchcombe, J.C., Barral, D.C., Mules, E.H., Booth, S., Hume, A.N., Machesky, L.M., Seabra, M.C., and Griffiths, G.M. (2001a). Rab27a is required for regulated secretion in cytotoxic T lymphocytes. J. Cell Biol. *152*, 825–834.

Stinchcombe, J.C., Bossi, G., Booth, S., and Griffiths, G.M. (2001b). The immunological synapse of CTL contains a secretory domain and membrane bridges. Immunity *15*, 751–761.

Sullivan, B.M., Juedes, A., Szabo, S.J., von Herrath, M., and Glimcher, L.H. (2003). Antigen-driven effector CD8 T cell function regulated by T-bet. Proc. Natl. Acad. Sci. USA *100*, 15818–15823.

Sumen, C., Mempel, T.R., Mazo, I.B., and Von Andrian, U.H. (2004). Intravital microscopy; visualizing immunity in context. Immunity *21*, 315–329.

Tang, Q., Henriksen, K.J., Bi, M., Finger, E.B., Szot, G., Ye, J., Masteller, E.L., McDevitt, H., Bonyhadi, M., and Bluestone, J.A. (2004). In vitro-expanded antigen-specific regulatory T cells suppress autoimmune diabetes. J. Exp. Med. *199*, 1455–1465.

Tang, Q., Adams, J.Y., Tooley, A.J., Bi, M., Fife, B.T., Serra, P., Santamaria, P., Locksley, R.M., Krummel, M.F., and Bluestone, J.A. (2006). Visualizing regulatory T cell control of autoimmune responses in nonobese diabetic mice. Nat. Immunol. *7*, 83–92.

Thomas, D.A., and Massague, J. (2005). TGF-beta directly targets cytotoxic T cell functions during tumor evasion of immune surveillance. Cancer Cell *8*, 369–380.

Trapani, J.A., and Smyth, M.J. (2002). Functional significance of the perforin/granzyme cell death pathway. Nat. Rev. Immunol. *2*, 735–747.

Turley, S., Poirot, L., Hattori, M., Benoist, C., and Mathis, D. (2003). Physiological beta cell death triggers priming of self-reactive T cells by dendritic cells in a type-1 diabetes model. J. Exp. Med. *198*, 1527–1537.

Waldmann, H., Graca, L., Cobbold, S., Adams, E., Tone, M., and Tone, Y. (2004). Regulatory T cells and organ transplantation. Semin. Immunol. *16*, 119–126.

Yang, Y., Huang, C.T., Huang, X., and Pardoll, D.M. (2004). Persistent Toll-like receptor signals are required for reversal of regulatory T cell-mediated CD8 tolerance. Nat. Immunol. *5*, 508–515.

Zelinskyy, G., Robertson, S.J., Schimmer, S., Messer, R.J., Hasenkrug, K.J., and Dittmer, U. (2005). CD8+ T-cell dysfunction due to cytolytic granule deficiency in persistent Friend retrovirus infection. J. Virol. *79*, 10619–10626.

Zippelius, A., Batard, P., Rubio-Godoy, V., Bioley, G., Lienard, D., Lejeune, F., Rimoldi, D., Guillaume, P., Meidenbauer, N., Mackensen, A., et al. (2004). Effector function of human tumor-specific CD8 T cells in melanoma lesions: a state of local functional tolerance. Cancer Res. *64*, 2865–2873.